2014

# R1234yf FLOW BOILING HEAT TRANSFER INSIDE A 3.4 mm ID MICROFIN TUBE

Andrea Diani
*University of Padova, Dept. of Industrial Engineering, Padova, 35131, Italy*, andrea.diani@studenti.unipd.it

Mariana Tiemi Tamura
*Departamento de Engenharia Mecânica, Universidade Federal de Santa Catarina, Florianópolis, SC, 88040-900, Brazil*, tamura.tiemi@gmail.com

Simone Mancin
*University of Padova, Dept. of Industrial Engineering, Padova, 35131, Italy*, simone.mancin@unipd.it

Jader Barbosa
*Departamento de Engenharia Mecânica, Universidade Federal de Santa Catarina, Florianópolis, SC, 88040-900, Brazil*, jrbpolo@gmail.com

Luisa Rossetto
*University of Padova, Dept. of Industrial Engineering, Padova, 35131, Italy*, luisa.rossetto@unipd.it

# R1234yf Flow Boiling Heat Transfer Inside a 3.4 mm ID Microfin Tube

Andrea DIANI[1], Mariana T. TAMURA[2], Simone MANCIN[1]*; Jader BARBOSA[2], Luisa ROSSETTO[1]

[1] University of Padova, Department of Industrial Engineering,
Padova, 35131, Italy. Ph.+39 0498276882, Fax +39 049 8276896
andrea.diani@unipd.it, simone.mancin@unipd.it, luisa.rosetto@unipd.it

[2] Universidade Federal de Santa Catarina, Departamento de Engenharia Mecânica
Florianópolis, SC, 88040-900, Brasil
tamura.tiemi@gmail.com, jrbpolo@gmail.com

* Corresponding author

## ABSTRACT

Refrigerant charge minimization as well as the use of eco-friendly fluids can be considered two of the most important targets for the next generation of air conditioning and refrigerating systems to cope with the new environmental regulations. Traditional microfin tubes are widely used in air and water heat exchangers for heat pump and refrigerating applications during either condensation or evaporation. The enhancement potential of microfin tubes can lead to more efficient and compact heat exchangers and thus to a reduction of the refrigerant charge of the systems. This paper explores the heat transfer and fluid flow characteristics of the new low-GWP refrigerant R1234yf during flow boiling inside a mini microfin tube with internal diameter at the fin tip of 3.4 mm. The microfin tube is brazed inside a copper plate and electrically heated from the bottom. Several T-type thermocouples are inserted in the wall to measure the temperature distribution during the phase change process. In particular, the experimental measurements were carried out at constant saturation temperature of 30 °C, by varying the refrigerant mass velocity between 190 kg $m^{-2}$ $s^{-1}$ and 940 kg $m^{-2}$ $s^{-1}$, the vapor quality from 0.2 to 0.99, at three different heat fluxes: 10, 25, and 50 kW $m^{-2}$. The experimental results are presented in terms of the two-phase heat transfer coefficient, onset of dryout vapor quality, and frictional pressure drop as a function of the operating test conditions.

## 1. INTRODUCTION

Recently, Domanski et al. (2013) and McLinden et al. (2013) have performed a detailed thermodynamic analysis of refrigerants, studying the performance limits of the vapour compression cycle and testing the possible low-GWP refrigerant candidates suitable for use in common types of refrigeration and air conditioning equipment. In particular, Domanski et al. (2013) suggested that the critical temperature of a refrigerant could be considered the most dominant parameter influencing the tradeoff between the coefficient of performance and the volumetric capacity. McLinden et al. (2013) carried out a screening of the possible refrigerants, eliminating those toxic or chemically unstable and focusing on those that presented critical temperatures between 300 K and 400 K; they analyzed 62 refrigerants. Two of those were R1234ze(E) and R1234yf, which have recently been the matter of research and investigation of the scientific community because of their negligible GWP and thermodynamic properties close to that of R134a, the fluid traditionally used in refrigeration and air conditioning equipment.
R1234yf has as a normal boiling temperature approximately 3.15 K lower than that of R134a and a GWP<1 whereas the normal boiling temperature of R1234ze(E) (GWP<1) is 7.3 K lower than that of R134a. These two fluids are candidates to substitute the more traditional R134a in several applications: from automotive air conditioning to high-temperature heat pumping.
Fukuda et al. (2014) thermodynamically, experimentally, and numerically analyzed the feasibility of R1234ze(E) and R1234ze(Z) for high-temperature heat pumps, demonstrating that these new low-GWP fluids are potential refrigerant substitutes in high-temperature heat pump systems also for industrial purposes, rather than typical air conditioners or refrigeration systems. However, to date, only few works experimentally investigated the heat transfer characteristics of these refrigerants during single and two-phase flow inside conventional and enhanced tubes.

Grauso et al. (2013) studied the heat transfer and pressure drop during evaporation of R1234ze(E) in an electrically heated circular smooth tube of 3 mm OD; the authors measured the two-phase heat transfer coefficient at different mass velocities, vapour qualities, and saturation temperatures between -2.9 °C and 12.1 °C ($p_{red}$= 0.05-0.09), imposing two different heat fluxes: 5 and 20 kW $m^{-2}$.

Del Col et al. (2013) investigated the R1234yf flow boiling heat transfer in a 1 mm diameter circular microchannel using water as secondary fluid. Flow boiling tests were carried out at 31 °C of saturation temperature ($p_{red}$ = 0.24), mass fluxes ranging between 200 and 600 kg $m^{-2}$ $s^{-1}$, and heat fluxes from 10 to 130 kW $m^{-2}$. The authors compared the results with those measured for R134a, and no significant differences between the flow boiling performance of R1234yf and R134a were reported.

Lu et al. (2013) investigated the effects of heat flux and mass flux on the two-phase convective boiling heat transfer performance for refrigerants R1234yf and R134a in a 3.9 mm ID smooth tube. The test section was a tube-in-tube heat exchanger with countercurrent water flow in the annulus, while the refrigerant evaporated inside the test tube. Tests were performed with a saturation temperature of 10 °C ($p_{red}$ = 0.13), with the mass velocity ranging from 200 to 500 kg $m^{-2}$ $s^{-1}$, and heat flux from 5 to 20 kW $m^{-2}$. A noticeable deterioration of the heat transfer coefficient for R1234yf was encountered and the pressure drops for R134a were about 5–15% higher than those for R1234yf.

Only one work related to flow boiling heat transfer of new low-GWP refrigerants inside microfin tubes has been found in the open literature; Kondou et al. (2013) experimentally investigated the flow boiling of R32, R1234ze(E) and R32/R1234ze(E) non-azeotropic mixtures in a horizontal microfin tube of 5.2 mm inner diameter at a saturation temperature of 10 °C (R32 $p_{red}$=0.19, R1234ze(E) $p_{red}$=0.09, R32/R1234ze(E) 0.2/0.8 $p_{red}$= 0.10; R32/R1234ze(E) 0.5/0.5 $p_{red}$=0.18). Water was used to vaporize the refrigerant and the heat flux was varied between 10 and 15 kW $m^{-2}$. The heat transfer coefficients of R1234ze(E) were lower than those of R32 but greater than those obtained for R32/R1234ze(E) mixtures.

A few of other works studied the flow boiling heat transfer inside microfin tubes with an internal diameter lower than 5 mm. Among those, one can cite Mancin et al. (2013a, 2013b, 2014), Gao et al. (2007a, 2007b), Dang et al. (2010), and Wu et al. (2013). Mancin et al. (2013a, 2013b, 2014) have experimentally investigated the flow boiling heat transfer of R134a inside an electrically heated mini microfin tube, with an internal diameter at the fin tip of 3.4 mm. The collected data permitted to study the effects of refrigerant mass velocity, vapour quality, and heat flux on the liquid-vapour phase change process at constant saturation temperature of 30 °C ($p_{red}$=0.19).

Gao et al. (2007a, 2007b) conducted experiments on flow boiling of $CO_2$-oil mixtures in electrically heated horizontal smooth and microfin tubes. The microfin tube was made of copper tube with an inner diameter of 3.04 mm. Experiments were carried out at mass velocities from 190 to 1300 kg $m^{-2}$ $s^{-1}$, at a saturation temperature of 10 °C ($p_{red}$=0.61), heat fluxes from 5 to 30 kW $m^{-2}$, and an oil circulation ratio from <0.01 to 0.72 wt%.

Dang et al. (2010) investigated the flow boiling of $CO_2$ inside an electrically heated internally-grooved tube, with an internal diameter of 2.0 mm at a saturation temperature of 15 °C ($p_{red}$=0.67), the heat flux ranged between 4.5 to 18 kW $m^{-2}$, and the mass velocity from 360 to 720 kg $m^{-2}$ $s^{-1}$. The heat transfer coefficient for the grooved tube was 1.9 - 2.3 times higher than that for the smooth tube, and the dryout quality was much higher, ranging between 0.90 and 0.95, while the pressure drops are 1.5 – 2.7 higher.

Wu et al. (2013) performed experiments during flow boiling of R22 and R410A inside one smooth tube and five microfin tubes with the same outer diameter of 5 mm, the mass velocity was varied from 100 to 620 kg $m^{-2}$ $s^{-1}$, the heat flux from 5 to 31 kW $m^{-2}$, at a saturation temperature of around 6 °C (R22 $p_{red}$ = 0.12; R134a $p_{red}$ = 0.20). The test section was a 2 m long horizontal tube-in-tube heat exchanger, where the refrigerant flowed in counter current with heating water. They also developed a new general semi-empirical model based on their own data and other data from open literature.

This paper presents the experimental results of R1234yf flow boiling heat transfer inside an electrically heated 3.4 mm ID microfin tube; the effects of mass flow rate, vapour quality, and heat flux on the two-phase heat transfer and pressure drop for a fixed saturation temperature of 30 °C are presented and analyzed.

## 2. EXPERIMENTAL SETUP

The experimental setup is located at the Heat Transfer in Micro-geometries Lab (HTMg-Lab) at the Dipartimento di Ingegneria Industriale of the University of Padova. As shown in Fig. 1, the experimental facility consists of three loops: refrigerant, cooling water and hot water loops. The rig was designed for heat transfer and pressure drop measurements and flow visualization during either vaporization or condensation of pure refrigerants and refrigerants mixtures inside structured micro-geometries. The facility has a maximum working pressure of 3 MPa, while refrigerant mass flow rate can be varied up to around 70 kg $h^{-1}$.

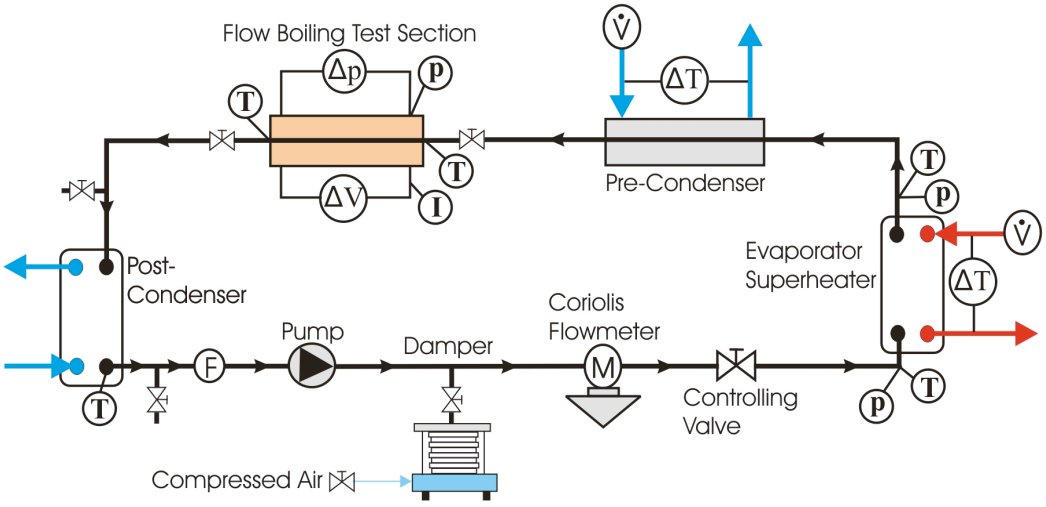


**Figure 1:** Schematic of the experimental setup.

In the first loop the refrigerant is pumped through the circuit by means of a magnetically coupled gear pump, it is vaporized and superheated in a brazed plate heat exchanger fed with hot water. Superheated vapour then partially condenses in a pre-condenser fed with cold water to achieve the set quality at the inlet of the test section. The refrigerant enters the test section at a known mass velocity and vapour quality and then it is vaporized by means of a calibrated Ni-Cr wire resistance. The fluid leaves the test section and enters in a post-condenser, a brazed plate heat exchanger, where it is fully condensed and subcooled. The subcooled liquid passes through a drier filter and then is sent back to the boiler by the pump. A damper connected to the compressed air line operates as pressure regulator to control the saturation condition in the refrigerant loop. As shown in Fig. 1, the refrigerant pressure and temperature are measured at several locations throughout the circuit to know the refrigerant properties at the inlet and outlet of each heat exchanger. The refrigerant mass flow rate can be independently controlled by the gear pump and it is measured by means of a Coriolis effect flowmeter. The inlet vapour quality to the test section is determined by the heat extracted in the precondenser, which can be controlled by varying the water temperature and flow rate. The cold water loop consists of a chiller with thermostatic control connected to the precondenser. The hot water circuit consists of a pump, an electrical heater and a controlling valve; it permits to set both the water flow rate and the inlet water temperature. Water flow rates in the precondenser and boiler sections are measured by means of magnetic type flow meters, while the water temperature differences are measured using 4-junction T-type thermopiles. Table 1 lists the values of accuracy of the instruments used in the experimental facility.

**Figure 2:** Photo of the test section.

**Table 1:** Values of the accuracy of the instruments used in the test rig.

| **Transducer** | **Accuracy** |
|---|---|
| T-type thermocouples | ± 0.05 K |
| T-type thermopiles | ± 0.03 K |
| Electric power | ± 0.13% of the reading |
| Coriolis mass flowmeter (refrigerant loop) | ± 0.10% of the reading |
| Magnetic volumetric flowmeters | ± 0.25% of the reading |
| Differential pressure transducer (test section) | ± 25 Pa |
| Absolute pressure transducers | ± 1950 Pa |

As shown in Fig. 2, the tested microfin tube is brazed inside a groove milled in a 20 mm thick, 10 mm wide, and 300 mm long copper plate. The pressure taps are located around 50 mm upstream and downstream of the heated tube; a smooth connection was designed and manufactured in order to prevent any possible abrupt pressure loss. The test tube has a heated length of 300 mm whereas the total length for the pressure drop measurement is 410 mm. The microfin tube is heated from the bottom by means of a calibrated Ni-Cr wire resistance inserted in a 2 mm deep groove milled on the bottom face of the copper plate. The heat is supplied by means of stabilized DC power supply rated up to 900 W. The instrumented test section is placed inside an aluminum housing filled with a 30 mm thick layer of rock wool to limit as much as possible the heat loss.
According to the nomenclature described in Fig. 3, the microfin tube has an OD of 4.0 mm, an ID at the fin's tip of $D$=3.4 mm, it has 40 fins with a height of $h$=0.12 mm, the helix angle $\beta$=18°. Twenty 1 mm ID holes were drilled along the centreline of the copper plate just 1 mm under the tested microfin tube. Twenty calibrated T-type thermocouples are inserted in those 5 mm deep holes to measure the wall temperature distribution during the heat transfer process. Figure 3 also presents a photo of the cross sectional area of the mini microfin tube tested where several fins are clearly visible.

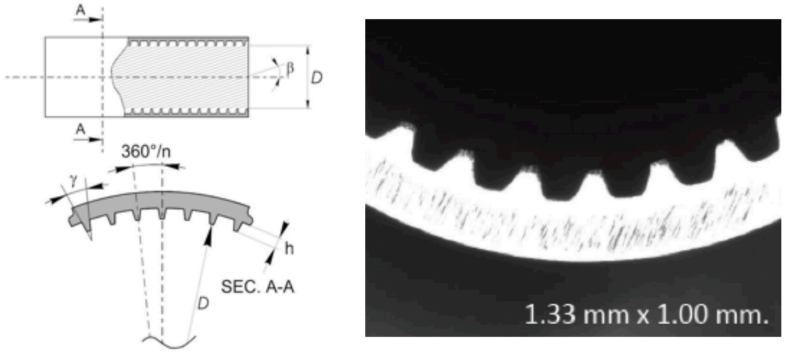


**Figure 3:** Drawing of a microfin tube (Cavallini et al., 2009) and photo of the cross section of the tested tube.

Preliminary heat transfer measurements permitted to estimate the heat loss ($q_{loss}$) due to conduction through the test section as a function of the mean wall temperature. The tests were run under vacuum conditions by supplying the power needed to maintain the mean wall temperature at a fixed value. The measurements were carried out by varying the wall temperature from around 30 °C to 60 °C, at different ambient temperatures from 21 °C to 24 °C. In this range, there was no appreciable effect of the ambient temperature on the actual heat loss. The results of these calibration tests are shown in Fig. 4, where the heat loss through the test section is plotted against the mean wall temperature.

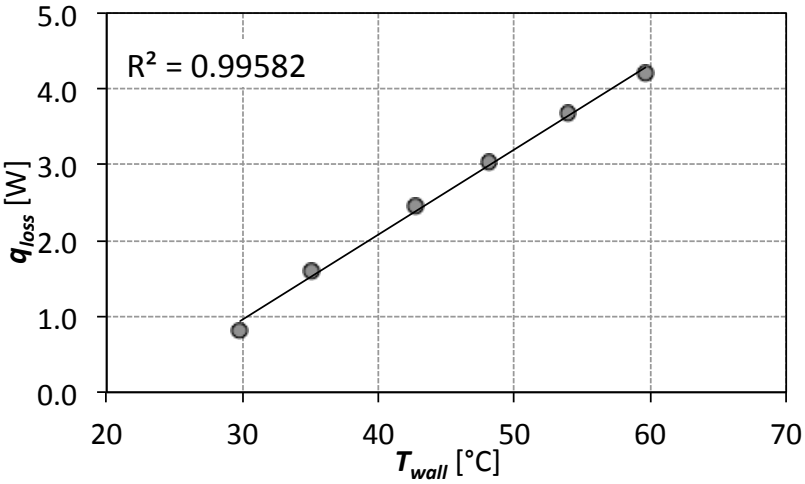


**Figure 4:** Measured values of the heat loss through the test section.

As it clearly appears the relationship between the heat loss and the wall temperature is linear; in this way, the actual value of heat supplied to the sample can be evaluated. The heat loss was never higher than 4% of the electrical power when the ambient temperature was kept constant within 21 °C and 24 °C.

## 3. DATA REDUCTION

As described before, the subcooled liquid is pumped to the boiler where it is vaporized and superheated; the refrigerant temperature and pressure are measured at both inlet and outlet of the heat exchanger. Preliminary tests were run to verify the heat balance at both the pre-condenser and evaporator; the deviation was always less than 2%. The vapour quality at the inlet of test section depends on the refrigerant conditions at the inlet of the pre-condenser and on the heat transfer rate exchanged in the tube-in-tube heat exchanger. It can be obtained from a thermal balance on the cooling water side given by:

$$q_{pc} = \dot{m}_{w,pc} \cdot c_{p,w} \cdot \left(t_{w,pc,out} - t_{w,pc,in}\right) = \dot{m}_{ref} \left(h_{vs} - h_{TS,in}\right) \tag{1}$$

where $\dot{m}_{w,pc}$ is the water mass flow rate at the precondenser, $c_{p,w}$ the water specific heat at constant pressure, $t_{w,pc,out}$ and $t_{w,pc,in}$ the water temperatures at the outlet and inlet of the precondenser, respectively. Considering the right-hand side of eq. (1), $\dot{m}_{ref}$ is the refrigerant mass flow rate, while $h_{vs}$ is the enthalpy of the superheated gas at the inlet of the pre-condenser, and $h_{TS,in}$ the enthalpy of the refrigerant at the inlet of the test section. The vapour quality at the inlet of the test section ($x_{in}$) can be calculated from the heat balance as:

$$x_{in} = \frac{h_{TS,in} - h_L}{h_V - h_L} \tag{2}$$

where $h_L$ and $h_V$ are the specific enthalpies of the saturated liquid and vapour, respectively, evaluated at the saturation pressure of the refrigerant measured at the inlet of the test section. All the thermophysical properties of the refrigerant were estimated using Refprop ver. 9.1 (Lemmon et al., 2013) database. The electrical power supplied to the sample is indirectly measured by means of a calibrated reference resistance (shunt) and by the measurement of the effective EDP (Electrical Difference Potential) of the resistance wire inserted in the copper heater. The current can be calculated from the Ohm's law. From preliminary measurements, the heat loss through the test section can be estimated by:

$$q_{loss}[\mathrm{W}] = 0.1121 \cdot \bar{t}_{wall}[^{\circ}\mathrm{C}] - 2.4042 \tag{3}$$

where $\bar{t}_{wall}$ is the mean wall temperature; thus, the actual heat flow rate supplied to the foam is given by:

$$q_{TS} = P_{EL} - q_{loss} = \Delta V \cdot I - q_{loss} \tag{4}$$

The two-phase heat transfer coefficient *HTC*, referred to the area of the smooth tube with the same inner diameter of that at the fin tip, $A_D$, can now be defined as:

$$HTC = \frac{q_{TS}}{A_D \cdot \left(\bar{t}_{wall} - \bar{t}_{sat}\right)} \tag{5}$$

where $\bar{t}_{wall}$ and $\bar{t}_{sat}$ are the average values of the wall and saturation temperatures, respectively. Their values are given by:

$$\bar{t}_{wall} = \frac{1}{20}\sum_{i=1}^{20} t_{wall,i} \qquad \bar{t}_{sat} = \frac{t_{sat,in}\left(p_{sat,in}\right) + t_{sat,out}\left(p_{sat,out}\right)}{2} \tag{6}$$

From the error propagation analysis, it was estimated that the mean uncertainty of the two-phase heat transfer coefficient is ±2.5%, whereas the vapour quality has an uncertainty of ±0.035.
The frictional pressure gradient is obtained from the measured value of the total pressure gradient by subtracting the momentum pressure gradient and neglecting the gravitational term, as given by:

$$\left(-\frac{dp}{dz}\right)_f = \left(-\frac{dp}{dz}\right)_{tot} - \left(-\frac{dp}{dz}\right)_M \tag{7}$$

The model proposed by the Rouhani and Axelsson (1970) was used to estimate the void fraction values to account for the momentum pressure gradient.

## 4. EXPERIMENTAL RESULTS

This paragraph presents the experimental results carried out during flow boiling heat transfer of R1234yf at a saturation temperature of 30 °C at the inlet of the test section for different heat fluxes, mass velocities, and vapour qualities. The experimental measurements are presented in terms of two-phase heat transfer coefficients and frictional pressure drops; the measurements also allow for the evaluation of the vapour quality at the onset of the dryout. As described before three different heat fluxes were investigated: 10, 25, and 50 kW m$^{-2}$ and the refrigerant mass velocity was varied from 190 to 940 kg m$^{-2}$ s$^{-1}$, while the vapour quality in the range $0.2<x_{mean}<0.99$. The heat flux is referred to the heat transfer area based on the outer diameter of the test tube, whereas the vapour quality variation in the test section ranged between 0.03 and 0.33, depending on the operating conditions.

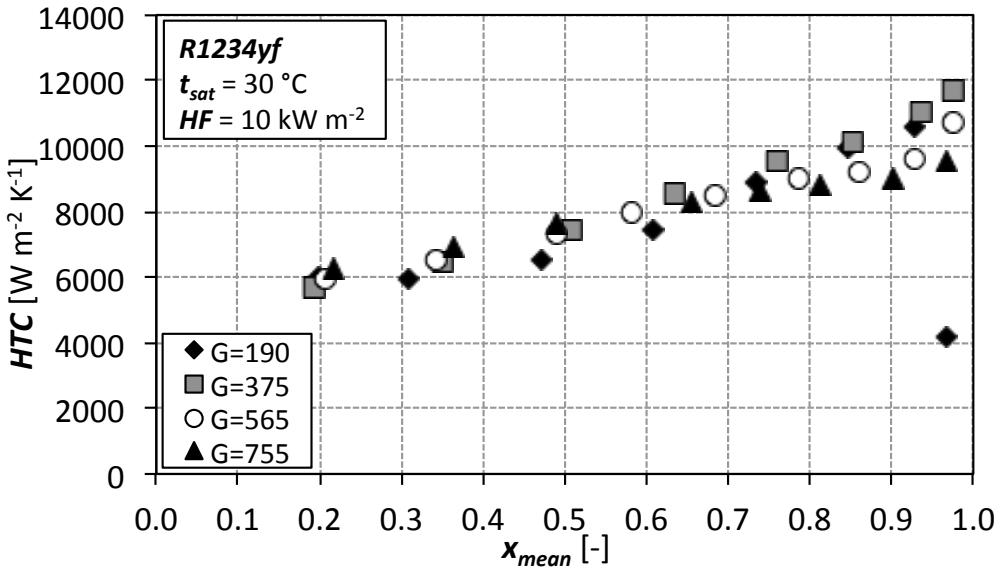


**Figure 5:** Effects of refrigerant mass velocity on flow boiling heat transfer at 10 kW m$^{-2}$. G [kg m$^{-2}$ s$^{-1}$]

Figure 5 shows the two-phase heat transfer coefficient plotted against the mean vapor quality at constant imposed heat flux of 10 kW m$^{-2}$. For G=190 kg m$^{-2}$ s$^{-1}$, the heat transfer coefficient shows a plateau of around 6000 W m$^{-2}$ K$^{-1}$. up to around $x_{mean}$=0.4. Then, the heat transfer coefficient increases with vapor quality, reaches a maximum value at around $x_{cr}$=0.93 and, finally, it suddenly decreases because the dryout phenomenon occurs. In this study, as suggested by Wojtan et al. (2005), the vapor quality at the onset of the dryout is determined as the last point before the heat transfer coefficient dropped more that 10% from its initial value. The behavior of *HTC* can be explained considering the two competing heat transfer mechanisms that control the phase change process: nucleate boiling and two-phase forced convection. In particular, at G=190 kg m$^{-2}$ s$^{-1}$, for $x_{mean}$<0.4, nucleate boiling seems to dominate the phase change process, whereas for higher values of vapor quality, the two-phase forced convection seems to become more effective. For higher mass velocities, the low-vapour quality heat transfer coefficient plateau disappears, and the two-phase heat transfer coefficient always increases with vapor quality meaning that the

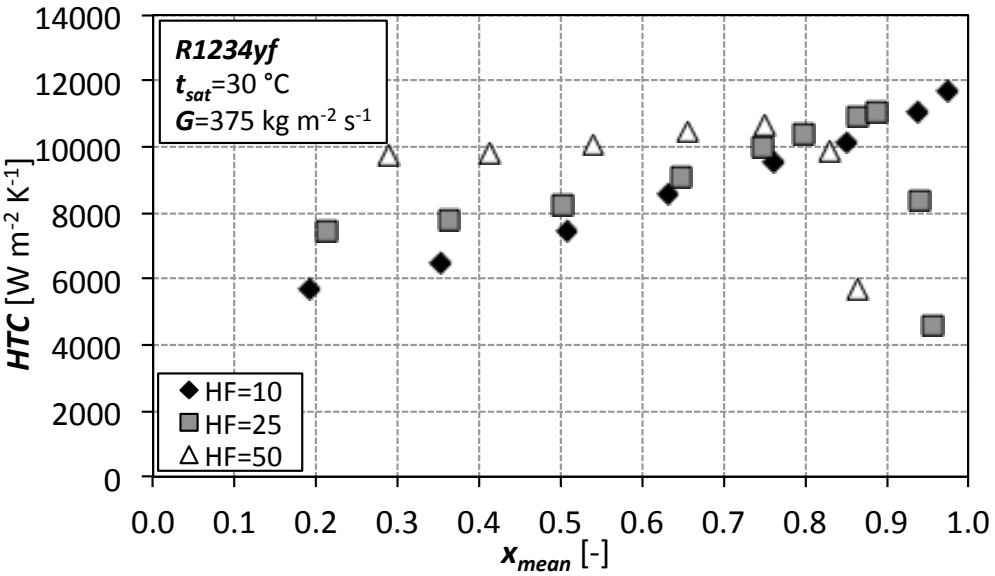


**Figure 6:** Effects of the heat flux on flow boiling heat transfer at G=375 kg m$^{-2}$ s$^{-1}$. HF [kW m$^{-2}$]

two-phase forced convection dominates the phase change process. Dryout did not occur at the higher mass velocities for a heat flux of 10 kW m$^{-2}$.

Still for the conditions of in Fig. 5, at low vapor qualities, the heat transfer coefficient exhibits almost the same values, whereas at high vapor quality, it increases as the mass velocity decreases. As already found by Mancin et al. (2014) for R134a, G=375 kg m$^{-2}$ s$^{-1}$ seems to be an optimal mass velocity showing the highest values of heat transfer coefficient. Figure 6 shows the heat transfer coefficient plotted against the mean vapour quality as a function of the heat flux at constant mass velocity of 375 kg m$^{-2}$ s$^{-1}$; it clearly appears that there is a strong relationship between the heat flux and the phase change process. In particular, at 10 and 25 kW m$^{-2}$, the heat transfer coefficient increases almost linearly with vapor quality; at the lowest imposed heat flux, the dryout phenomenon does not occur, while at 25 kW m$^{-2}$ the thermal crisis starts at around $x_{cr}$=0.91. The heat transfer coefficient increases as the heat flux increases, up to around $x_{mean}$=0.65, while at higher vapor qualities, the heat transfer enhancement becomes lower. At HF=50 kW m$^{-2}$, the heat transfer coefficient does not depend on vapour quality being almost constant at around 10000 W m$^{-2}$ K$^{-1}$.

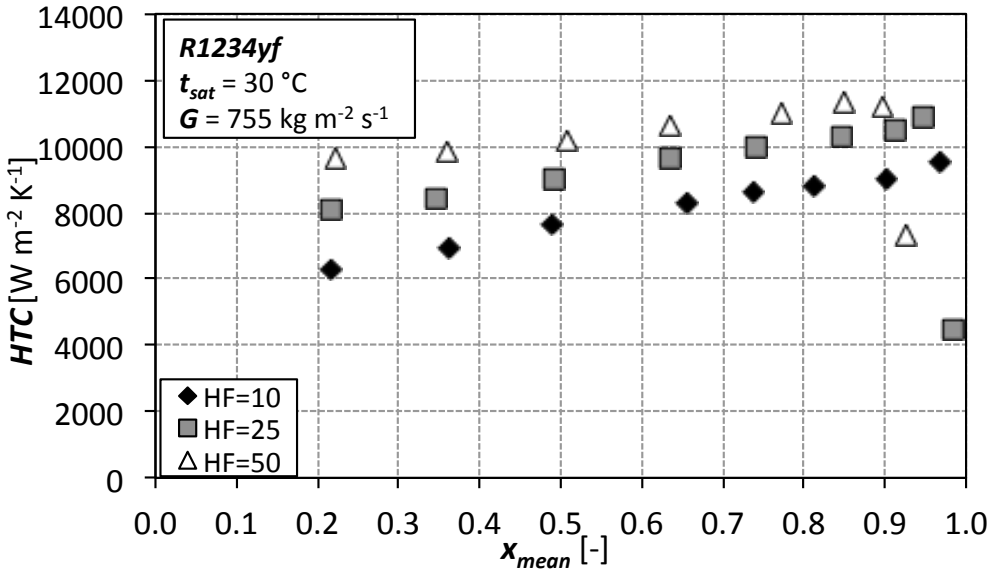


**Figure 7:** Effects of the heat flux on flow boiling heat transfer at G=755 kg m$^{-2}$ s$^{-1}$. HF [kW m$^{-2}$]

This behavior can be explained considering the two competing mechanisms that control the phase change process: nucleate boiling and two-phase forced convection. At low heat flux, the flow boiling heat transfer is influenced by the two-phase forced convection, in fact the heat transfer coefficient increases with the vapor quality. For higher heat fluxes, especially at low vapor quality, the nucleate boiling becomes more important and dominates the phase change process. In this region, there is a direct relationship between the heat flux and the heat transfer coefficient. As the vapor quality increases, the nucleate boiling mechanism also seems to be suppressed by the two-phase forced convection; the heat transfer coefficients before the dryout inception for 10, 25, and 50 kW $m^{-2}$ are quiet similar. Finally, it can be noticed that at HF=25 kW $m^{-2}$ and HF=50 kW $m^{-2}$, the dryout phenomenon occurs and the vapor quality at its onset decreases as the heat flux increases passing from around $x_{cr}$=0.91 to around $x_{cr}$=0.81, respectively.

Figure 7 presents the same diagram plotted in Figure 6 but data were carried out at higher mass velocity, G=755 kg $m^{-2}$ $s^{-1}$; at these operating test conditions, the nucleate boiling and the two-phase forced convection show a synergistic behavior rather than competitive. The heat transfer coefficient increases when increasing both mass velocity and heat flux. A small plateau where the heat transfer coefficient is almost constant can be noticed at HF=50 kW $m^{-2}$ for $x_{mean}$<0.5 but then heat transfer coefficient increases with vapor quality. As already mentioned, the dryout phenomenon does not occur at HF=10 kW $m^{-2}$ while it occurs at 25 and 50 kW $m^{-2}$ at $x_{cr}$=0.95 and $x_{cr}$=0.89, respectively.

The diagram plotted in Figure 8 shows the effects of the mass velocity and vapor quality on the two-phase frictional pressure gradients; the Rouhani and Axelsson (1970) model was used to estimate the void fraction values to account for the momentum pressure gradient. The results show that, at constant mass velocity, the frictional pressure gradient increases with vapor quality, reaching a maximum value and, then, it decreases following the well-known behavior during two-phase flow. Finally, at constant vapor quality, the frictional pressure gradient increases as the mass velocity increases.

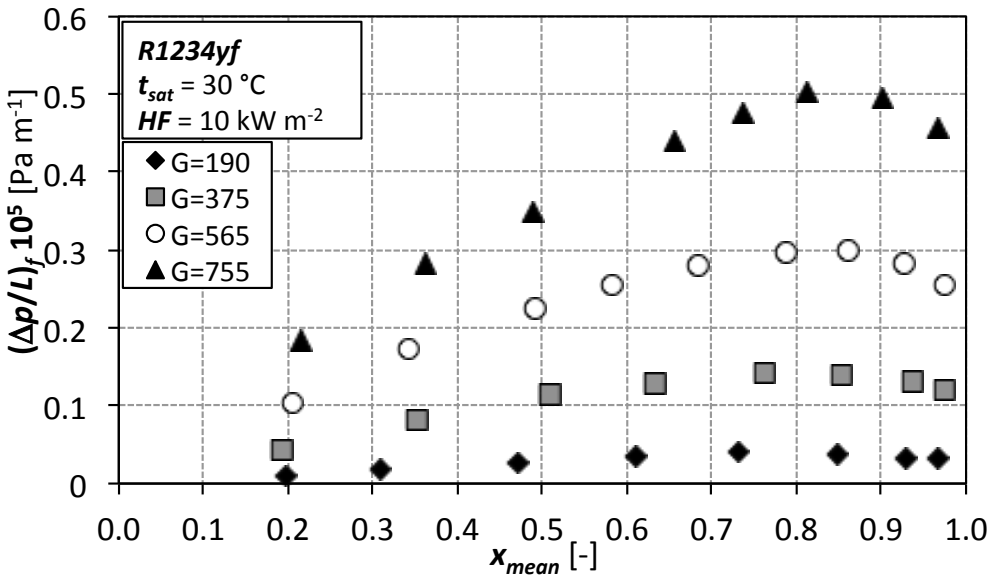


**Figure 8:** Frictional pressure drops measured at 10 kW $m^{-2}$. G [kg $m^{-2}$ $s^{-1}$]

## 5. CONCLUSIONS

This paper presented experimental results carried out during R1234yf flow boiling heat transfer inside a mini microfin tube having an internal diameter at the fin tip of 3.4 mm. The measurements were conducted at constant saturation temperature of 30 °C at the tube inlet by varying the refrigerant mass velocity between 190 kg $m^{-2}$ $s^{-1}$ and 940 kg $m^{-2}$ $s^{-1}$ and the vapor quality from 0.2 to 0.99; three different heat fluxes were investigated: 10, 25, and 50 kW $m^{-2}$. The results show that the flow boiling heat transfer is controlled by the two well-know phase change heat transfer mechanisms: nucleate boiling and two-phase forced convection. At constant saturation temperature, the actual operating conditions: heat flux, vapor quality, and mass velocity determine which of those dominates the

phase change process. The developed measuring technique permits to find the vapor quality at the onset of the dryout, which occurs at different values depending on the operating test conditions. At a heat flux of 10 kW $m^{-2}$, the dryout phenomenon only occurs at G=190 kg $m^{-2}$ $s^{-1}$ whereas at higher mass velocity no thermal crisis was observed. When increasing the heat flux, it is possible to identify the value of the vapor quality at the onset of dryout; for a given mass velocity, this value decreases as the heat flux increases. The frictional pressure gradients were also presented; the results show the effect of the vapor quality and mass velocity. In fact, the pressure gradient increases with both these two parameters. These results highlight the promising heat transfer capabilities of mini microfin tubes during flow boiling heat transfer as well as the interesting heat transfer properties of this new low-GWP refrigerant. The results obtained for R1234yf can be compared with those measured during flow boiling inside the same tube as reported in Mancin et al. (2013a, 2013b, 2014). The R1234yf shows similar heat transfer coefficients at 10 kW $m^{-2}$, whereas it exhibits higher heat transfer capabilities at 25 and 50 kW $m^{-2}$. The frictional pressure drop values for the two refrigerants are similar.

## NOMENCLATURE

| | | |
|---|---|---|
| $A_D$ | heat transfer area | ($m^2$) |
| $c_p$ | specific heat at constant p | (J $kg^{-1}$ $K^{-1}$) |
| -dp/dz | pressure gradient | (Pa $m^{-1}$) |
| $G$ | mass velocity | (kg $m^{-2}$ $s^{-1}$) |
| $h$ | specific enthalpy | (J $kg^{-1}$) |
| | fin height | (m) |
| $HF$ | heat flux | (W $m^{-2}$) |
| $HTC$ | heat transfer coefficient | (W $m^{-2}$ $K^{-1}$) |
| $I$ | electric current | (A) |
| $L$ | sample length | (m) |
| $\dot{m}$ | mass flow rate | (kg $s^{-1}$) |
| $n$ | number of fins | (-) |
| $p$ | pressure | (Pa) |
| $P_{EL}$ | electrical power | (W) |
| $q$ | heat flow rate | (W) |
| $t$ | temperature | (°C) |
| $x$ | quality | (-) |

Greek symbols

| | | |
|---|---|---|
| $\beta$ | helix angle | (°) |
| $\Delta T$ | temperature difference | (K) |
| $\Delta V$ | electric potential | (V) |
| $\gamma$ | apex angle | (°) |

Subscripts

| | |
|---|---|
| a | momentum term |
| cr | critical |
| f | frictional |
| in | inlet |
| L | saturated liquid |
| loss | loss |
| mean | mean |
| out | outlet |
| pc | precondenser |
| ref | refrigerant |
| red | reduced |
| sat | saturation |
| tot | total |
| TS | test section |
| V | saturated vapor |

| | |
|---|---|
| vs | superheated vapor |
| w | water |
| wall | wall |

## REFERENCES


Cavallini, A., Del Col, D., Mancin, S., Rossetto, L., 2009, Condensation of pure and near-azeotropic refrigerants in microfin tubes: A new computational procedure. *Int. J. Refrig.,* vol. 32, p. 162-174.

Dang, C., Haraguchi, N., Hihara, E., 2010, Flow boiling heat transfer of carbon dioxide inside a small-size microfin tube. *Int. J. Refrig.,* vol. 33, p. 655-663.

Del Col, D., Bortolin, S., Rossetto, L., 2013. Convective boiling inside a single circular microchannel. *Int. J. Heat and Mass Transf.,* vol. 67, p. 1231-1245.

Domanski, P.A., Brown, J.S., Heo, J., Wojtusiak, J., Mc Linden, M.O., 2013. A thermodynamic analysis of refrigerants: Performance limits of the vapor compression cycle. *Int. J. Refrig.,* DOI:10.1016/j.ijrefrig.2013.09.036

Fujie, K., Itoh, N., Kimura, H., Nakayama, N., Yanugidi, T., 1977, Heat transfer pipe. US Patent 4044797, assigned to Hitachi LTD.

Fukuda, S., Kondou, C., Takata, N., Koyama, S., 2014, Low GWP refrigerants R1234ze(E) and R1234ze(Z) for high temperature heat pumps. *Int. J. Refrig.,* vol. 40, p. 161–173.

Gao, L., Honda, T., Koyama, S., 2007, Experiments on Flow Boiling Heat Transfer of Almost Pure CO2 and CO2-Oil Mixtures in Horizontal Smooth and Microfin Tubes. *HVAC&R Research*, vol. 13, p. 415-425.

Gao, L., Ono, T., Honda, T., 2007. Pressure drops of $CO_2$ and oil mixtures in horizontal smooth and micro-fin tube evaporators. *Proc. of International Congress of Refrigeration,* Beijing, ICR07-B1-1262.

Grauso, S., Mastrullo, R., Mauro, A.W., Thome, J.R., Vanoli, G.P., 2013, Flow pattern map, heat transfer and pressure drops during evaporation of R-1234ze(E) and R134a in a horizontal, circular smooth tube: Experiments and assessment of predictive methods. *Int. J. Refrig.,* vol. 36, p. 478-491.

Han, D., Lee, K.J., 2005. Experimental study on condensation heat transfer enhancement and pressure drop penalty factors in four microfin tubes. Int. J. Heat Mass Transf., vol. 48, p. 3804-3816.

Kondou, C., BaBa, D., Mishima, F., Koyama, S, 2013, Flow boiling of non-azeotropic mixture R32/R1234ze(E) in horizontal microfin tubes. Int. J. Refrigeration 36, 2366-2378.

Lemmon, E.W., Huber, M.L., McLinden, M.O., 2013, NIST Standard Reference Database 23: Reference Fluid Thermodynamic and Transport Properties-REFPROP, Version 9.1, National Institute of Standards and Technology, Standard Reference Data Program, Gaithersburg.

Lu, M.C., Tong, J.R., Wang, C.C., 2013, Investigation of the two-phase convective boiling of HFO-1234yf in a 3.9 mm diameter tube. *Int. J. of Heat and Mass Transf.,* vol. 65, p. 545–551.

Mancin, S., Diani, A., Zilio, C., Rossetto, L., 2013a, Experimental Measurements of R134a Flow Boiling Inside a 3.4 mm ID Microfin Tube. Proc. of 13th UK Heat Transfer Conference, UKHTC2013, 2 - 3 September, Imperial College London, UK.

Mancin, S., Diani, D., Rossetto, L., 2013b, Experimental Measurements of R134a Flow Boiling Inside a 3.4 mm ID Microfin Tube. Submitted to *Heat Transfer Engineering*.

Mancin, S., Diani, A., Rossetto, L., 2014, R134a Flow Boiling Heat Transfer and Pressure Drop inside a 3.4 mm ID Microfin Tube. *Energy Procedia*, vol. 45, p. 608–615.

Mc Linden, M.O., Kazanov, A.F., Brown, J.S., Domanski, P.A., 2013, A Thermodynamic Analysis of Refrigerants: Possibilities and Tradeoffs for Low-GWP Refrigerants. *Int. J. Refrig.*, DOI/10.1016/j.ijrefrig.2013.09.032.

Rouhani, S.Z., Axelsson, E., 1970. Calculation of void volume fraction in the subcooled and quality boiling regions. *Int. J. Heat Mass Transf.,* vol. 13, p. 383-393.

Wojtan, L., Ursenbacher, T., Thome, J.R., 2005, Investigation of flow boiling in horizontal tubes: Part I-A new diabatic two-phase flow pattern map. *Int. J. Heat Mass Transf.,* vol. 48, p. 2955-2969.

Wu, Z., Wu. Y., Sunden, B., Li, W., 2013, Convective vaporization in micro-fin tubes of different geometries. *Exp. Therm. Fluid Sc.*, vol. 44, p. 298-408.


## ACKNOWLEDGEMENT

The support of Wieland-Werke AG, Dr. Christoph Walther, and University of Padova on this research activity is gratefully acknowledged.